Annals of Nuclear Energy 85 (2015) 788–797

Contents lists available at ScienceDirect

Annals of Nuclear Energy

journal homepage: www.elsevier.com/locate/anucene

Code development for eigenvalue total sensitivity analysis and total uncertainty analysis

Chenghui Wan [a], Liangzhi Cao [a], Hongchun Wu [a], Tiejun Zu [a,*], Wei Shen [a,b]

[a] Xi'an Jiaotong University, Xi'an, Shaanxi, China
[b] Canadian Nuclear Safety Commission, Ottawa, Ontario, Canada

ARTICLE INFO

Article history:
Received 25 March 2015
Received in revised form 21 June 2015
Accepted 26 June 2015
Available online 9 July 2015

Keywords:
Sensitivity analysis
Uncertainty analysis
Implicit effects
Cross sections

ABSTRACT

The uncertainties of multigroup cross sections notably impact eigenvalue of neutron-transport equation. We report on a total sensitivity analysis and total uncertainty analysis code named UNICORN that has been developed by applying the direct numerical perturbation method and statistical sampling method. In order to consider the contributions of various basic cross sections and the implicit effects which are indirect results of multigroup cross sections through resonance self-shielding calculation, an improved multigroup cross-section perturbation model is developed. The DRAGON 4.0 code, with application of WIMSD-4 format library, is used by UNICORN to carry out the resonance self-shielding and neutron-transport calculations. In addition, the bootstrap technique has been applied to the statistical sampling method in UNICORN to obtain much steadier and more reliable uncertainty results. The UNICORN code has been verified against TSUNAMI-1D by analyzing the case of TMI-1 pin-cell. The numerical results show that the total uncertainty of eigenvalue caused by cross sections can reach up to be about 0.72%. Therefore the contributions of the basic cross sections and their implicit effects are not negligible.

1. Introduction

In recent years, there has been an increasing demand for best estimate predictions to be provided with their confidence bounds in many domains, including nuclear research, industry, safety and regulation (Ivanov et al., 2013). Uncertainty analysis is a proper way to determine the appropriate design margins. The neutronics calculations are prerequisite for the predictions of reactor system, and the uncertainties introduced by neutronics calculations would be propagated to the subsequent calculations, such as thermal/hydraulics, neutron kinetics and safety analysis. Therefore, uncertainty analysis for neutronics calculations is the basic analysis in reactor design. Recently, the imprecision of cross sections, which would introduce uncertainties to responses of neutronics calculations, has been treated as one of the most significant sources of uncertainty (Pusa, 2012). According to the previous researches, the relative standard deviations of the eigenvalue caused by cross-section uncertainties are significant and non-ignorable (Wieselquist et al., 2012; Yankov et al., 2012). In this context, it's necessary to perform uncertainty analysis for neutronics calculations to obtain much more confident and appropriate safety margins introduced by cross-section uncertainties.

In order to perform the uncertainty propagations from nuclear cross sections to the responses of neutronics calculations, two categories of methodologies have been widely applied: the deterministic method and the statistical sampling method. For the deterministic method, sensitivity analysis is implemented firstly to obtain the sensitivity coefficients of responses with respect to cross sections. Perturbation theory (PT) (Weisbin et al., 1976; Pusa, 2012) and direct numerical perturbation (DNP) (Rearden, 2009) method are widely used to perform the sensitivity analysis. After the sensitivity coefficients are obtained, uncertainties of responses can be calculated by applying the "sandwich rule" (Rearden et al., 2009) combining sensitivity coefficients with corresponding covariance matrix of the cross sections. For the statistical sampling method, samples of cross sections are generated from their distributions regions firstly. The cross-section samples are then used as input parameters to carry out the neutronics calculations to obtain the responses of interest with respect to corresponding cross-section samples. Finally, the statistical calculation is applied to calculate the uncertainties of responses.

There are two important problems which should be considered when performing sensitivity and uncertainty analysis for responses with respect to cross sections. Firstly, in neutronics

* Corresponding author at: No. 28 Xianning West Road, Xi'an 710049, China. Tel.: +86 029 82663285; fax: +86 029 82667802.
E-mail address: tiejun@mail.xjtu.edu.cn (T. Zu).

http://dx.doi.org/10.1016/j.anucene.2015.06.036
0306-4549/

calculations, only the integral cross sections, such as the total cross section σ_t and scattering cross section σ_s are required, while the basic cross sections like $\sigma_{(n,\mathrm{elas})}$, $\sigma_{(n,2n)}$, $\sigma_{(n,\gamma)}$ and so forth are not directly used. However, the uncertainties of these basic cross sections can also cause uncertainties to the responses. Therefore, the analysis should be performed not only to the integral cross sections, including σ_t, σ_s and σ_a, but also to the basic cross sections, including $\sigma_{(n,\mathrm{elas})}$, $\sigma_{(n,\mathrm{inel})}$, $\sigma_{(n,2n)}$, $\sigma_{(n,3n)}$, $\sigma_{(n,f)}$, $\sigma_{(n,\gamma)}$, $\sigma_{(n,p)}$, $\sigma_{(n,D)}$, $\sigma_{(n,T)}$, $\sigma_{(n,\mathrm{He})}$, $\sigma_{(n,\alpha)}$ and ν.

Secondly, the effects of cross sections on the responses can be divided into two parts: the explicit portion and the implicit portion. This phenomenon is due to the fact that in deterministic method for neutronics calculation, both resonance self-shielding and neutron-transport calculations are required. The explicit portion is defined as the direct contributions of effective self-shielding cross sections on the responses through neutron-transport calculation. The implicit portions are the contributions of cross sections on responses through resonance self-shielding calculation. And the total effect is defined as summation of the explicit portion and implicit portion. It has been observed that the implicit portions are important and non-ignorable (Rearden et al., 2005). There are two categories of methodologies having been applied to consider the implicit portions. The first one focuses on resonance self-shielding calculation model, such as works done by Liu et al. (2015), Rearden et al. (2009), Foad and Takeda (2015) and Dion and Marleau (2013). The other one focuses on the multigroup cross-section library and cross-section perturbation models have been established, such as works done by Ball et al. (2013) and Kinoshita et al. (2014).

In order to consider the two aspects of works above, a new code named UNICORN, performing the total sensitivity analysis and total uncertainty analysis for eigenvalue with respect to cross sections, has been developed in this paper. To consider the implicit effects of cross sections to eigenvalue, the method applied in the UNICORN code is chosen focusing on the multigroup cross-section library. This method has the advantage of convenient practice and a multigroup cross-section perturbation model is required. Ball et al. (2013) has proposed a multigroup cross-section perturbation model, with which total sensitivity analysis can be performed for eigenvalue to the cross sections stored in the WIMSD-4 format library. However, total sensitivity analysis to various basic cross sections which are important to sensitivity and uncertainty analysis, are beyond the capability of this model. Therefore, the improvements, including the perturbation propagations and consistency rules for various basic cross sections, have been accomplished to the multigroup cross-section perturbation model. With the improved cross-section perturbation model, the UNICORN code has the capability of performing total sensitivity analysis and total uncertainty analysis for the eigenvalue with respect to all types of integral and basic cross sections mentioned above. Moreover, some conclusions about detailed origins of the implicit effects, which haven't been published before, are laid out in this work from the neutron physics point of view.

The statistical sampling method and DNP method have been chosen and accomplished in the UNICORN code to perform sensitivity and uncertainty analysis. For uncertainty analysis, the statistical sampling method has the obvious advantages including convenience, no approximation and no limit to the number of responses, compared with the deterministic method. However, the sensitivity coefficients, which are essential elements for sensitivity analysis, can't be obtained by the statistical sampling method. However, the sensitivity coefficients are important and essential for similarity analysis (Rearden and Jessee, 2009), and cross-section adjustment (Broadhead et al., 2004). Therefore, in order to perform sensitivity analysis, the DNP method has been selected and accomplished in the UNICORN code. In the context, the desirable features of DNP method and statistical sampling method have been incorporated in the UNICORN code to perform total sensitivity analysis and total uncertainty analysis respectively. In addition, the lattice code DRAGON 4.0 (Marleau et al., 2014) is used to carry out the resonance self-shielding calculation and neutron-transport calculation with application of the WIMSD-4 format multigroup cross-section library.

An overview of the UNICORN code is given in Section 2. In sequences, Section 3–5 describe the multigroup cross-section perturbation model, statistical sampling method and direct numerical perturbation method, respectively. In Section 6, verification of the UNICORN code is given and the corresponding numerical results and analysis are presented.

2. Overview of the UNICORN code

In this paper, the UNICORN code has been developed to perform total sensitivity analysis and total uncertainty analysis for the eigenvalue of neutronics calculations with respect to the multigroup cross sections. The flowchart of the UNICORN code is shown in Fig. 1.

In the UNICORN code, the basic models include these three parts: the multigroup cross-section perturbation model (described in Section 3), the statistical sampling method (described in Section 4) and the direct numerical perturbation method (described in Section 5). The nuclear data which is necessary, including all types of integral and basic cross sections, are obtained by incorporating the WIMSD-4 format library and the output of NJOY (Macfarlane et al., 2012). Based on the nuclear data and basic models, the UNICORN code has the capability of detailed sensitivity and uncertainty analysis for various kinds of cross sections.

3. Multigroup cross-section perturbation model

In order to consider the basic cross sections and implicit effects mentioned above, the multigroup cross-section perturbation model proposed by Ball et al. (2013) has been improved in this paper. This section will describe the improved multigroup cross-section perturbation model in detail. This section consists of three parts: firstly, the generations of multigroup cross sections and resonance integrals from point-wise cross sections are introduced as the basic theory for the multigroup cross-section perturbation model; secondly, the perturbation propagations from the point-wise cross sections to the multigroup ones and resonance integrals are introduced; finally, the consistency rules between the integral and basic cross sections are explained.

3.1. Multigroup cross sections and resonance integrals

The cross sections in ENDF files should be processed to specific multigroup format, e.g. the WIMSD-4 format, before they can be utilized by the deterministic lattice code, such as DRAGON. The energy- and temperature-dependent point-wise cross sections are converted into specific multigroup format using weighting flux $\phi(E,\sigma_0)$ shown as the following formula:

$$\sigma_{x,g}(T,\sigma_0)=\frac{\int_{\Delta E_g}\sigma_x(E,T)\phi(E,\sigma_0)dE}{\int_{\Delta E_g}\phi(E,\sigma_0)dE} \tag{1}$$

where T, E and σ_0 represent the temperature, energy and background cross section respectively. And $\sigma_x(E,T)$ stands for the energy- and temperature-dependent point-wise cross sections. For the non-resonance cross sections, the weighting flux is the function of energy (formulated as $\phi(E)$), and for the cross sections with resonances, the weighting flux is relative to both energy and

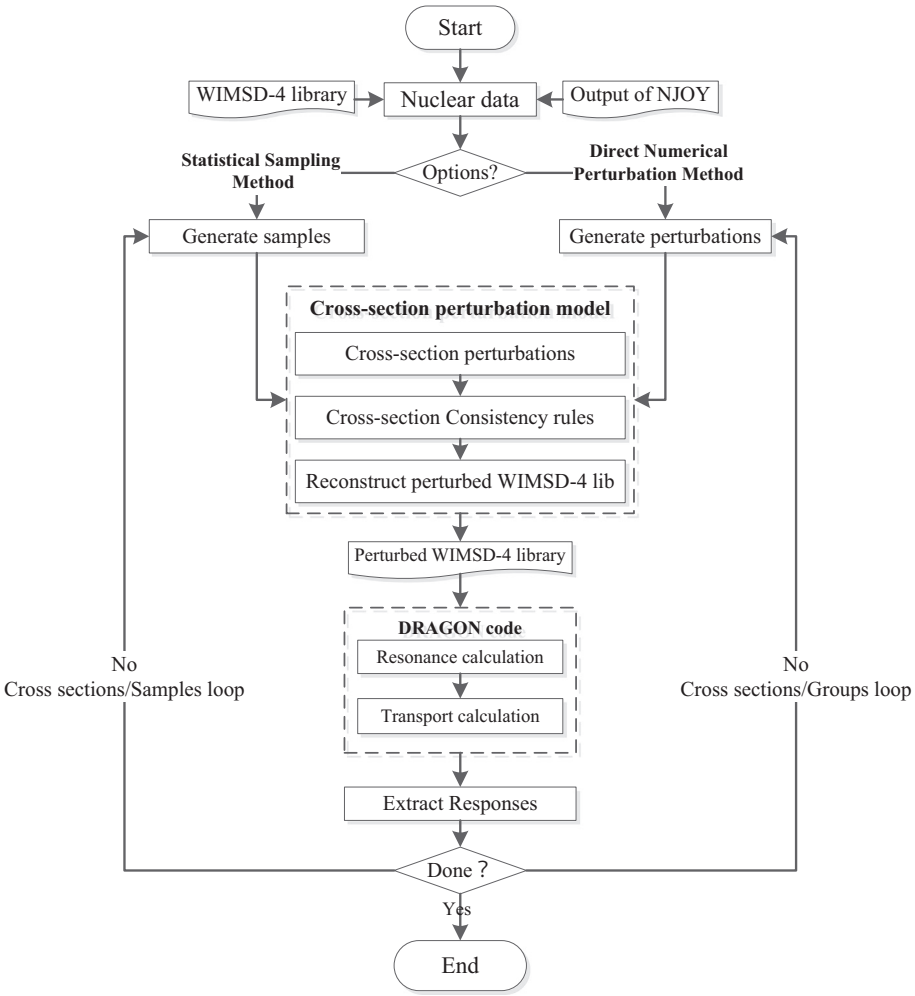

Fig. 1. Flowchart of the UNICORN code.

background cross sections. And for convenience, the weighting flux is presented as $\phi(E,\sigma_0)$ in following.

Generally, the NJOY code is used to generate the multigroup cross-section library. With respect to the weighting flux $\phi(E,\sigma_0)$, the users can either choose one of the options for the *iwt* parameter of the GROUPR module in the NJOY code, or input it through the input file of NJOY. Whichever way is chosen, slowing-down equation should be solved for a homogeneous mixture of the resonant absorber with non-resonance nuclides to obtain the weighting flux within the resonance-energy region for the resonant cross sections. With application of the narrow resonance (NR) approximation (Leszczynski et al., 2007), the weighting flux $\phi(E,\sigma_0)$ within resonance regions can be presented as shown in Eq. (2):

$$\phi(E,\sigma_0) = \frac{\sigma_p^r + \sigma_0}{\sigma_t(E) + \sigma_0}\Psi(E) \tag{2}$$

where σ_p^r and $\sigma_t(E)$ present the potential scattering cross section and total cross section of the resonant nuclide correspondingly, and $\Psi(E)$ stands for the $1/E$ shape. The multigroup resonance cross sections can be obtained by substituting Eq. (2) into Eq. (1).

According to WIMSD-4 format multigroup library (Leszczynski et al., 2007), the relations between the resonance cross sections and corresponding resonance integrals for the gth group of cross sections of type x can be formulated as shown in Eq. (3):

$$\sigma_{x,g}(T,\sigma_b) = \frac{I_{x,g}(T,\sigma_b)\sigma_b}{\sigma_b - I_{a,g}(T,\sigma_b)} \tag{3}$$

where σ_b is defined as sum of σ_p^r and σ_0; $\sigma_{a,g}(T,\sigma_b)$ and $I_{x,g}(T,\sigma_b)$ present the resonance absorption cross section and resonance integral of type x, at temperature T and background cross section σ_0. By applying Eq. (3), the tables of resonance integrals, stored in WIMSD-4 format library, can be converted to the tables of resonance cross sections which are required for analysis in this paper.

3.2. Perturbation propagations

The multigroup cross-section perturbation model is established based on WIMSD-4 format library to take into account of the implicit effects. Since the multigroup cross sections are generated from the point-wise cross sections, the multigroup cross-section perturbations should be consistency with the perturbations propagated from the point-wise cross sections. In this paper, it is assumed that the perturbation for the gth group of type x is performed by the uniform relative perturbation to the point-wise cross section within the energy range of the gth group, shown as in Eq. (4):

$$\sigma_x'(E,T) = (1+\delta_{x,g})\sigma_x(E,T) \quad E_{g-1} \le E \le E_g \tag{4}$$

where E_{g-1} and E_g present the lower and upper energy boundaries of the gth group; $\sigma_x'(E,T)$ stands for the perturbed point-wise cross section of type x.

For the cross sections without resonance, the weighting flux is selected or input by users and independent of the point-wise cross sections. Therefore, the perturbation propagations from the

point-wise cross sections to the multigroup ones are linear and can be presented shown as in Eq. (5):

$$\sigma'_{x,g}(T) = \frac{\int_{\Delta E_g} \sigma'_x(E,T)\phi(E)dE}{\int_{\Delta E_g} \phi(E)dE} = (1+\delta_{x,g})\frac{\int_{\Delta E_g} \sigma_x(E,T)\phi(E)dE}{\int_{\Delta E_g} \phi(E)dE} = (1+\delta_{x,g})\sigma_{x,g}(T) \quad (5)$$

However, for the resonant cross sections, the perturbation propagations are non-linear. Because the weighting flux within resonance-energy regions would be perturbed at the same time due to perturbations to the point-wise cross sections, according to Eq. (2). Therefore, strict derivation should be performed to determine the correct propagations of perturbations from the point-wise cross sections to the multigroup ones.

Substituting the Eq. (4) into Eqs. (1) and (2), and the perturbed resonant cross sections can be written as:

$$\begin{aligned}\sigma'_{x,g}(T,\sigma_0) &= \frac{\int_{\Delta E_g} \sigma'_x(E,T)\phi(E,\sigma_0)dE}{\int_{\Delta E_g} \phi(E,\sigma_0)dE} \\ &= (1+\delta_{x,g})\frac{\int_{\Delta E_\mu} \sigma_x(\mu,T)\frac{\sigma_p^r+\sigma_0}{\sigma_t(\mu,T)+\delta_{x,g}\sigma_x(\mu,T)+\sigma_0}d\mu}{\int_{\Delta E_\mu}\frac{\sigma_p^r+\sigma_0}{\sigma_t(\mu,T)+\delta_{x,g}\sigma_x(\mu,T)+\sigma_0}d\mu} \\ &= (1+\delta_{x,g})\frac{\int_{\Delta E_\mu} \sigma_x(\mu,T)\frac{\sigma_p^r+\sigma_0}{(1+\delta_{t,g})\sigma_t(\mu,T)+\sigma_0}d\mu}{\int_{\Delta E_\mu}\frac{\sigma_p^r+\sigma_0}{(1+\delta_{t,g})\sigma_t(\mu,T)+\sigma_0}d\mu} \\ &= (1+\delta_{x,g})\sigma_{x,g}(T,\sigma'_0) \end{aligned} \quad (6)$$

where σ'_0 stands for the perturbed background cross sections due to perturbations of point-wise cross sections which can be expressed as shown in Eq. (7):

$$\sigma'_0 = \frac{\sigma_0}{1+\delta_{t,g}} \quad (7)$$

where $\delta_{t,g}$ presents the relative perturbation of total cross section due to the relative perturbations $\delta_{x,g}$ of type x. The perturbed resonant cross sections can be converted into corresponding resonance integrals by application of Eq. (8):

$$I'_{x,g}(T,\sigma_b) = \frac{\sigma'_{x,g}(T,\sigma_b)\sigma_b}{\sigma'_{a,g}(T,\sigma_b)+\sigma_b} \quad (8)$$

3.3. Consistency rules

In this paper, total sensitivity analysis and total uncertainty analysis have been accomplished to not only the integral cross sections including σ_t, σ_s and σ_a, but also the basic cross sections including $\sigma_{(n,\mathrm{elas})}$, $\sigma_{(n,\mathrm{inel})}$, $\sigma_{(n,2n)}$ and so forth, which are absent from neutron-transport equation and lumped in the integral cross sections. In order to perform the total sensitivity analysis and total uncertainty analysis for the basic cross sections absent from neutron-transport equation, the consistency rules should be established to achieve the goal that the individual perturbation of basic cross sections could be propagated and presented in the integral ones. According to the WIMSD-4 format multigroup library, the scattering, absorption and total cross sections are defined as shown in Eqs. (9)–(11) respectively.

$$\sigma_{s,g\to h} = \sigma_{(n,\mathrm{elas}),g\to h} + \sigma_{(n,\mathrm{inel}),g\to h} + 2\sigma_{(n,2n),g\to h} + 3\sigma_{(n,3n),g\to h} \quad (9)$$

$$\sigma_{a,g} = \sigma_{(n,f)} + \sigma_{(n,g)} + \sigma_{(n,\alpha)} + \sigma_{(n,2\alpha)} + \sigma_{(n,p)} + \sigma_{(n,D)} + \sigma_{(n,T)} + \sigma_{(n,\mathrm{He3})} - \sigma_{(n,2n),g} - 2\sigma_{(n,3n),g} \quad (10)$$

$$\sigma_{t,g} = \sigma_{a,g} + \sigma_{s,g} \quad (11)$$

According to these formulas, integral cross sections are dependent on corresponding basic cross sections, for example σ_a is dependent on the basic cross sections $\sigma_{(n,f)}$, $\sigma_{(n,\gamma)}$ and so forth as shown in Eq. (10). Hence, the consistency rules for different types of cross sections are presented in Table 1–3.

In Tables 1–3, σ_s, σ_a, σ_{vf} and σ_{tr} present the scattering, absorption, fission yield and transport cross sections respectively; I_a and I_{vf} stand for resonance integrals of absorption and fission yield cross sections. Table 1 is used to propagate perturbations of basic cross sections without resonance nuclides like ^{16}O and ^{1}H, and can also be used to the thermal and fast groups for resonant nuclides. Perturbation propagation of basic resonant cross sections within the resonance groups should apply Table 2. Table 3 is used in case of non-resonance cross sections for resonant nuclides such as $\sigma_{(n,\mathrm{elas})}$ of ^{235}U within resonance groups, because σ_t would be perturbed and thus the resonance cross sections would be perturbed according to Eqs. (6) and (7). For integral cross sections, including σ_s, σ_a and σ_t, perturbations to these cross sections can be converted to perturbations to corresponding basic cross sections uniformly. For example, when relative perturbation $\delta_{a,g}$ is applied to the gth group of absorption cross section, the same relative perturbation, $\delta_{a,g}$ is added to all basic cross sections present in Eq. (10) and relative perturbation propagations are considered according to Tables 1–3. It should be noted that when perturbation is achieved to σ_a (or σ_s), σ_s (or σ_a) should not be perturbed, because $\sigma_{(n,2n)}$ and $\sigma_{(n,3n)}$ are contributors both to σ_a and σ_s as shown in Eqs. (9) and (10).

Based on the cross-section perturbation propagations and consistency rules described above, the WIMSD-4 format multigroup library can be perturbed, reconstructed and rewritten to perform total sensitivity analysis and total uncertainty analysis for eigenvalue with respect to the basic and integral cross sections.

4. Statistical sampling method

Statistical sampling method is widely applied to perform uncertainty analysis for complex system with multi-inputs and multi-responses. Therefore, in the UNICORN code, the statistical sampling method is an option to perform total uncertainty analysis. In this section, the basic theory and method of the statistical sampling method is introduced.

4.1. Theory and method

For any system, the relationship between input parameters and responses can be briefly characterized as shown in Eq. (12):

$$\boldsymbol{R} = \boldsymbol{f}(\boldsymbol{X}) \quad (12)$$

where $\boldsymbol{X}$ presents the multi-input vector and can be characterized as $\boldsymbol{X} = [x_1, x_2, \ldots, x_{nX}]^T$ in which nX is the number of input parameters; $\boldsymbol{R}$ presents the multi-response vector and can be characterized as $\boldsymbol{R} = [R_1, R_2, \ldots, R_{nR}]^T$ in which nR is the number of responses.

There are three main steps to perform uncertainty propagation from the uncertainties of input parameters to the responses (Helton et al., 2006): firstly, determine the distribution ranges of input parameters; secondly, generate the samples of the input parameters; finally, statistical calculation for responses of corresponding input samples.

In the first step, the uncertainties of input parameters are required. In this paper, the interested input parameters are cross sections, and the uncertainties of cross sections can be characterized by the group-wise covariance matrix. The covariance matrix for input parameters characterized as $\boldsymbol{X}$ can be defined as $\boldsymbol{\Sigma}$. As to the covariance matrix $\boldsymbol{\Sigma}$, the diagonal elements present the variances or uncertainties of input parameters, and the off diagonal elements are covariance between different input parameters, characterizing the correlations between them. Combined with the expectation vector $\boldsymbol{\mu}$ which is characterized as $\boldsymbol{\mu} = [\mu_1, \mu_2, \ldots, \mu_{nX}]^T$ for $\boldsymbol{X}$, the distribution ranges for every input parameter can be determined.

Table 1
Cross-section perturbations to basic cross sections without resonance in WIMSD-4 library.

Basic cross sections	Cross-section perturbations	Cross-section consistency rules
$\sigma_{(n,x)}(x = \text{elas,inel})$	$\sigma'_{(n,x),g} = (1 + \delta_{x,g})\sigma_{(n,x),g}$	$\sigma'_{s,g} = \sigma_{s,g} + \delta_{x,g}\sigma_{(n,x),g}$ $\sigma'_{tr,g} = \sigma_{tr,g} + \delta_{x,g}\sigma_{(n,x),g}$
$\sigma_{(n,2n)}$	$\sigma'_{(n,2n),g} = (1 + \delta_{(n,2n),g})\sigma_{(n,2n),g}$	$\sigma'_{s,g} = \sigma_{s,g} + 2\delta_{(n,2n),g}\sigma_{(n,2n),g}$ $\sigma'_{a,g} = \sigma_{a,g} - \delta_{(n,2n),g}\sigma_{(n,2n),g}$ $\sigma'_{tr,g} = \sigma_{tr,g} + \delta_{(n,2n),g}\sigma_{(n,2n),g}$
$\sigma_{(n,3n)}$	$\sigma'_{(n,3n),g} = (1 + \delta_{(n,3n),g})\sigma_{(n,3n),g}$	$\sigma'_{s,g} = \sigma_{s,g} + 3\delta_{(n,3n),g}\sigma_{(n,3n),g}$ $\sigma'_{a,g} = \sigma_{a,g} - 2\delta_{(n,3n),g}\sigma_{(n,3n),g}$ $\sigma'_{tr,g} = \sigma_{tr,g} + \delta_{(n,3n),g}\sigma_{(n,3n),g}$
$\sigma_{(n,x)}(x = \text{p,D,T,He},\alpha,2\alpha)$	$\sigma'_{(n,x),g} = (1 + \delta_{x,g})\sigma_{(n,x),g}$	$\sigma'_{a,g} = \sigma_{a,g} + \delta_{x,g}\sigma_{(n,x),g}$ $\sigma'_{tr,g} = \sigma_{tr,g} + \delta_{x,g}\sigma_{(n,x),g}$

Table 2
Cross-section perturbations to basic cross sections with resonances in WIMSD-4 library.

Basic cross sections	Cross-section perturbations	Cross-section consistency rules
$\sigma_{(n,f)}$	$\sigma'_{(n,f),g} = (1 + \delta_{(n,f),g})\sigma_{(n,f),g}$	$\sigma'_{tr,g} = \sigma_{tr,g} + \delta_{(n,f),g}\sigma_{(n,f),g}$ $\sigma'_{a,g} = \sigma_{a,g} + \delta_{(n,f),g}\sigma_{(n,f),g}$ $\sigma_{vf,g} = \upsilon\,(1 + \delta_{(n,f),g})\sigma_{(n,f),g}$ $I'_{a,g}(T,\sigma_0) = \sigma'_{a,g}(T,\sigma'_0)\sigma_0/$ $(\sigma'_{a,g}(T,\sigma'_0) + \sigma_0)$ $I'_{vf,g} = \sigma'_{vf,g}(T,\sigma'_0)\sigma_0/$ $(\sigma'_{a,g}(T,\sigma'_0) + \sigma_0)$
$\sigma_{(n,\gamma)}$	$\sigma'_{(n,\gamma),g} = (1 + \delta_{(n,\gamma),g})\sigma_{(n,\gamma),g}$	$\sigma'_{tr,g} = \sigma_{tr,g} + \delta_{(n,\gamma),g}\sigma_{(n,\gamma),g}$ $\sigma'_{a,g} = \sigma_{a,g} + \delta_{(n,\gamma),g}\sigma_{(n,\gamma),g}$ $I'_{a,g}(T,\sigma_0) = \sigma'_{a,g}(T,\sigma'_0)\sigma_0/$ $(\sigma'_{a,g}(T,\sigma'_0) + \sigma_0)$ $I'_{vf,g} = \sigma_{vf,g}(T,\sigma'_0)\sigma_0/$ $(\sigma'_{a,g}(T,\sigma'_0) + \sigma_0)$

In the second step, it is complicated to generate the samples directly by application of the covariance matrix $\boldsymbol{\Sigma}$, because different input parameters such as x_i and x_j can be dependent, and thus samples for one parameter should consider the union effects to the others parameters. For this reason, samples for the dependent parameters can be inverted to those for independent parameters by application of the Eq. (13):

$$\boldsymbol{X}_S = \boldsymbol{\Sigma}^{1/2}\boldsymbol{Y}_S + \boldsymbol{\mu} \tag{13}$$

where $\boldsymbol{X}_s$ presents the sample space for $\boldsymbol{X}$; $\boldsymbol{Y}_s$ presents the sample space for $\boldsymbol{Y}$ which has the same dimension with $\boldsymbol{X}$, and all parameters of $\boldsymbol{Y}$ are independent and obey standard normal distributions; $\boldsymbol{\Sigma}^{1/2}$ is the square root of covariance $\boldsymbol{\Sigma}$. $\boldsymbol{X}_s$ and $\boldsymbol{Y}_s$ have the same dimension nX^*nS in which nS is the number of samples for each parameter of $\boldsymbol{X}$ and $\boldsymbol{Y}$. It is quite practical and convenient to generate the independent samples $\boldsymbol{Y}_s$, based on which the dependent samples $\boldsymbol{X}_s$ for parameters $\boldsymbol{X}$ can be obtained according to Eq. (13).

In the third step, results of uncertainty analysis are obtained by application of statistical calculation for the responses of all samples. When the sample of input parameters $\boldsymbol{X}_{s,i}$, which can be characterized as $\boldsymbol{X}_{s,i} = [x_{1,i}, x_{2,i},\ldots, x_{nX,i}]^T$ $(i = 1,2,\ldots, nS)$, is used as input to carry out response calculations, the corresponding responses of the system can be presented as R_i. So, the mapping $[\boldsymbol{X}_{s,i},R_i]$ for $i = 1,2,\ldots, nS$ can be obtained. And the uncertainties of responses are obtained by application of statistical calculation as shown in Eq. (14):

$$\sigma(R) = \sqrt{\frac{1}{nS-1}\sum_{i=1}^{nS}(R_i - R_0)^2} \tag{14}$$

where $\sigma(R)$ stands for standard deviation of response and R_0 presents the expectation value of response and is characterized as shown in Eq. (15):

$$R_0 = \frac{1}{nS}\sum_{i=1}^{nS}R_i \tag{15}$$

By applications the three main steps above, the uncertainty of eigenvalue due to these of multigroup cross sections can be obtained.

For the statistical sampling method, the sampling technology selection is an important part. There are three different sampling technologies (Helton and Davis, 2002): Random Sampling (RS), Stratified Sampling (SS) and Latin Hypercube Sampling (LHS). RS is the easiest technologies to generate samples, with the disadvantage that there is no assurance that the sample elements can cover all subsets of distribution space for $\boldsymbol{X}$. SS can ensure that the sample elements can cover all subsets of distribution space but has the disadvantage that the strata and strata probabilities should be determined, which makes it complicated to perform the uncertainty analysis applying samples with different probabilities. LHS technology incorporates the desirable features of RS and SS. The implementation of LHS technology is easier than that of SS because it is not necessary to determine the strata and corresponding probabilities, and each sample has the same probability like RS which makes it practical and convenient to perform the uncertainty analysis. Arguably, LHS technology is one of the best small-sample statistical sampling approaches for uncertainty analysis. Therefore, LHS technology is applied to generate samples for input parameters in this study.

Table 3
Cross-section perturbations to total cross sections within resonance groups in WIMSD-4 library.

Cross sections	Cross-section perturbations	Cross-section consistency rules
σ_t	$\sigma'_{t,g} = (1 + \delta_{t,g})\sigma_{t,g}$	$I'_{a,g}(T,\sigma_0) = \sigma_{a,g}(T,\sigma'_0)\sigma_0/$ $(\sigma_{a,g}(T,\sigma'_0) + \sigma_0)$ $I'_{vf,g} = \sigma_{vf,g}(T,\sigma'_0)\sigma_0/(\sigma_{a,g}(T,\sigma'_0) + \sigma_0)$

4.2. Bootstrap method for confidence interval

The statistical errors are inevitable to the uncertainty results because the number of samples is a specific but infinite number. To enhance the reliability and confidence of uncertainties results, the bootstrap method has been applied to evaluate the confidence intervals for the uncertainty results (Archer et al., 1997). For the purpose to evaluate confidence interval for uncertainties results of uncertainty analysis, resampling technology is used and series of re-samples are generated to perform the uncertainty analysis. The response uncertainty of ith re-samples can be presented as $\sigma(R)_i$ $(i = 1,2,\ldots,N)$ where N is the total number of re-samples,

and the bootstrap confidence interval can be quantified by formula as Eq. (16) shown:

$$\Delta\sigma(R) = \sqrt{\frac{1}{N-1}\sum_{i=1}^{N}(\sigma(R)_i - \sigma(R)_0)^2} \tag{16}$$

where $\Delta\sigma(R)$ presents the deviation of the uncertainty results by application of the N re-samples; $\sigma(R)_i$ is the uncertainty result of the ith re-samples, and $\sigma(R)_0$ presents the expectation value of the N uncertainty results which can be formulated shown as in Eq. (17):

$$\sigma(R)_0 = \frac{1}{N}\sum_{i=1}^{N}\sigma(R)_i \tag{17}$$

By applications of Eqs. (16) and (17), the confidence intervals for uncertainty results can be quantified and the uncertainty results can be much more confident and reliable with the limited size of samples.

5. Direct numerical perturbation method

The DNP method is a straightforward and convenient method to perform sensitivity and uncertainty analysis. In the UNICORN code, the DNP method is an alternative method to perform the total sensitivity analysis and total uncertainty analysis of eigenvalue on multigroup cross sections. This method can overcome the disadvantage of the statistical sampling method which doesn't have the capability of calculating the sensitivity coefficients.

5.1. Sensitivity analysis

The relative sensitivity coefficients of eigenvalue to multigroup cross sections estimated by the DNP method can be presented briefly as shown in Eq. (18), and DNP method is a straightforward numerical method applying difference quotient to estimate the partial derivative:

$$\begin{aligned} S_{k,\sigma_{x,g}} &= \frac{\sigma_{x,g}}{k}\frac{\partial k}{\partial \sigma_{x,g}} \approx \frac{\sigma_{x,g}}{k}\frac{k((1+\delta^+_{x,g})\sigma_{x,g}) - k((1+\delta^-_{x,g})\sigma_{x,g})}{(\delta^+_{x,g}-\delta^-_{x,g})\sigma_{x,g}} \\ &= \frac{1}{k}\frac{k((1+\delta^+_{x,g})\sigma_{x,g}) - k((1+\delta^-_{x,g})\sigma_{x,g})}{\delta^+_{x,g}-\delta^-_{x,g}} \end{aligned} \tag{18}$$

where $\sigma^+_{x,g}$ and $\sigma^-_{x,g}$ represent the positive and negative relative perturbations for the gth group's cross section with type of x respectively; $\sigma_{x,g}$ and k stand for the un-perturbed cross section and eigenvalue respectively. The Eq. (18) is a brief formula in which only the cross sections under analysis are presented and the other input parameters are treated as constants without perturbation, and thus absent from the equation. When Eq. (18) is used, one issue should be noted: to ensure the numerical accuracy, the relative perturbations of cross sections should be as much as small, but taking the effects of truncation of computation into account, the relative perturbations of cross sections should not be too small. It is obvious that with respect to an NG groups cross sections library, 2^*NG physics calculations should be carried out, with NG for positive perturbations and the other NG for negative perturbations. The group-wise relative sensitivity coefficient vector of eigenvalue with respect to cross sections will be obtained by application of sensitivity analysis, and the vector has the dimension of n^*NG where n presents the number of cross sections under analysis.

5.2. Uncertainty analysis

Uncertainty analysis can be performed by combining the relative sensitivity coefficients with relative covariance matrix based on the "sandwich rule". The "sandwich rule" for uncertainty quantification of eigenvalue to the multigroup cross sections can be presented as shown in Eq. (19):

$$\frac{\sigma^2(k)}{k^2} = \boldsymbol{S}_{k,\alpha_i}\boldsymbol{\Sigma}_{\alpha_i\alpha_j}\boldsymbol{S}^T_{k,\alpha_j} \tag{19}$$

where $\sigma^2(k)$ is the variance of eigenvalue which presents the uncertainty results of eigenvalue due to uncertainties of multigroup cross sections; $\boldsymbol{S}_{k,\alpha_i}$ and $\boldsymbol{S}_{k,\alpha_j}$ stand for the relative sensitivity coefficients vectors of eigenvalue to multigroup cross sections; α_i and α_j can present any type of cross sections for any group; $\boldsymbol{\Sigma}_{\alpha_i\alpha_j}$ presents the relative covariance data for cross sections α_i and α_j.

6. Numerical results and analysis

In this section, the UNICORN code has been verified against the TSUNAMI code. The TMI-1 pin-cell case, one of the UAM ("Uncertainty Analysis in Modeling") (Ivanov et al., 2013) benchmarks, has been analyzed by the both codes. And two aspects of verification have been done. Firstly, the verification for total sensitivity analysis is carried out by comparing the relative sensitivity coefficients of the UNICORN code with those of TSUANMI. This part of verification is also aimed at verifying the correctness of the multigroup cross-section perturbation model. Secondly, the verification for the total uncertainty analysis is performed through comparing the uncertainty results of eigenvalue to different types of cross sections by the statistical sampling method with those by the DNP method.

6.1. Verification for total sensitivity analysis

In order to verify the results of total sensitivity analysis using the DNP method, TSUNAMI-1D (Rearden et al., 2009) is applied to perform total sensitivity analysis to the same case of TMI-1 pin-cell. The NR approximation has been applied both by TSUNAMI-1D and UNICORN for the implicit effects analysis. The difference between TSUNAMI-1D and UNICORN is the methodology applied when considering the cross-section implicit effects, for which TSUNAMI-1D uses the perturbation theory, while UNICORN applies the DNP method. Therefore, the TSUNAMI-1D code has been selected as the standard code to verify the UNICORN code in this paper.

For the purpose to reduce the difference of UNICORN between the TSUNAMI-1D, 1D calculation for neutron-transport equation is carried out by both TSUNAMI-1D and DRAGON 4.0 in UNICORN. And the 172-group library used by UNICORN is generated from the ENDF/B-VII.0 library because the v7-238 library applied by TSUNAMI-1D is also based on ENDF/B-VII.0 library.

Total sensitivity analysis of the lattice multiplication constant, k_∞ with respect to multigroup cross sections has been performed. The relative perturbation size of all nuclides and types of cross sections is set to 0.1% uniformly in UNICORN. The fifteen most significant cross-section sources of uncertainties in the case of TMI-1 pin-cell and corresponding energy-integrated total relative sensitivity coefficients by TSUNAMI-1D and UNICORN are compared and shown in Table 4.

According to Table 4, the results of the total sensitivity analysis by the UNICORN code agree well with those of TSUNAMI-1D. Therefore, the multigroup cross-section perturbation model can be proven correct and so does the development of the UNICORN code for total sensitivity analysis using the DNP method.

As mentioned above, the implicit portion of sensitivity coefficients, which is defined as differences of the total relative sensitivity coefficients with the explicit ones, are very important in some groups, and the implicit contributions are researched and analyzed

Table 4
Energy-integrated total relative sensitivity coefficients for the fifteen most significant cross-section sources of uncertainties.

Nuclides	Cross sections	TSUNAMI	UNICORN
^{235}U	ν	9.4165E−01	9.4049E−01
^{235}U	$\sigma_{(n,f)}$	2.5314E−01	2.5243E−01
^{238}U	$\sigma_{(n,\gamma)}$	−2.1230E−01	−2.2039E−01
^{1}H	$\sigma_{(n,\mathrm{elas})}$	1.7877E−01	1.7516E−01
^{235}U	$\sigma_{(n,\gamma)}$	−1.5512E−01	−1.5472E−01
^{238}U	ν	5.8352E−02	5.9515E−02
^{1}H	$\sigma_{(n,\gamma)}$	−3.7695E−02	−3.7763E−02
^{238}U	$\sigma_{(n,f)}$	2.7824E−02	2.8268E−02
^{16}O	$\sigma_{(n,\mathrm{elas})}$	−9.7846E−03	−1.1293E−02
^{238}U	$\sigma_{(n,\mathrm{inel})}$	−5.6771E−03	−5.7531E−03
^{91}Zr	$\sigma_{(n,\gamma)}$	−4.2938E−03	−4.2917E−03
^{16}O	$\sigma_{(n,\alpha)}$	−3.1924E−03	−3.3620E−03
^{92}Zr	$\sigma_{(n,\gamma)}$	−1.4406E−03	−1.4854E−03
^{90}Zr	$\sigma_{(n,\gamma)}$	−1.3336E−03	−1.4106E−03
^{238}U	$\sigma_{(n,2n)}$	1.0877E−03	1.1648E−03

by comparing the total and explicit relative sensitivity coefficients in this study. And the explicit relative sensitivity coefficients are obtained by perturbing the effective self-shielding multigroup cross sections, also by using the DNP method. The energy-integrated explicit and total relative sensitivity coefficients are compared and shown in Table 5.

It can be observed that the differences between the total and explicit relative sensitivity coefficients, the implicit portions, exist only for some types of cross sections. For much more detailed comparisons analysis of the implicit portions in the total relative sensitivity coefficients, the group-wise relative sensitivity coefficients have been compared for some representative types of cross sections shown as in Fig. 2.

By comparisons of the explicit and total group-wise relative sensitivity coefficients as shown in Fig. 2, it can be observed that the implicit contributions are caused by the resonances groups (from the 46th to 92nd groups for the 172-groups energy structure) and can be caused by either the $\sigma_{(n,\mathrm{elas})}$ of non-resonance nuclides or $\sigma_{(n,\mathrm{elas})}$, $\sigma_{(n,f)}$ and $\sigma_{(n,\gamma)}$ of the resonant nuclides. These observations can be explained as following.

Firstly, for $\sigma_{(n,\gamma)}$ of ^{238}U shown in Fig. 2 (a), the implicit portions play positive contributions in the total relative sensitivity coefficients. This can be explained like this. For the total sensitivity analysis, when 1% positive relative perturbation has been added to $\sigma_{(n,\gamma)}$ of ^{238}U within the resonance groups, the actual perturbation to the effective self-shielding $\sigma_{(n,\gamma)}$ would be less than 1%, which can be explained with application of Eqs. (6) and (7). According to Eq. (7), positive relative perturbation would result in decrease

Table 5
The energy-integrated explicit and total relative sensitivity coefficients.

Nuclides	Cross sections	Explicit	Total
^{235}U	ν	9.4049E−01	9.4049E−01
^{235}U	$\sigma_{(n,f)}$	2.5365E−01	2.5243E−01
^{238}U	$\sigma_{(n,\gamma)}$	−2.3741E−01	−2.2039E−01
^{1}H	$\sigma_{(n,\mathrm{elas})}$	1.8627E−01	1.7516E−01
^{235}U	$\sigma_{(n,\gamma)}$	−1.5393E−01	−1.5472E−01
^{238}U	ν	5.9512E−02	5.9515E−02
^{1}H	$\sigma_{(n,\gamma)}$	−3.7761E−02	−3.7763E−02
^{238}U	$\sigma_{(n,f)}$	2.8268E−02	2.8268E−02
^{16}O	$\sigma_{(n,\mathrm{elas})}$	−1.4184E−03	−1.1293E−02
^{238}U	$\sigma_{(n,\mathrm{inel})}$	−5.7370E−03	−5.7531E−03
^{91}Zr	$\sigma_{(n,\gamma)}$	−4.2417E−03	−4.2917E−03
^{16}O	$\sigma_{(n,\alpha)}$	−3.3601E−03	−3.3620E−03
^{92}Zr	$\sigma_{(n,\gamma)}$	−1.4644E−03	−1.4854E−03
^{90}Zr	$\sigma_{(n,\gamma)}$	−1.3766E−03	−1.4106E−03
^{238}U	$\sigma_{(n,2n)}$	1.1574E−03	1.1648E−03

to the background cross sections, so the values increase to the resonance table for σ_a (for ^{238}U, only the $\sigma_{(n,\gamma)}$ has resonance and the $\sigma_{(n,f)}$ is small and without resonance) would be less than 1% according to Eq. (6). However, for the explicit sensitivity analysis, the relative increase of effective self-shielding $\sigma_{(n,\gamma)}$ would be exactly 1%, because the perturbation is added directly to the effective self-shielding multigroup cross sections. According to the neutron-transport equation, smaller absorption cross section (for the total sensitivity analysis) would result in larger k_∞. Therefore, the relative sensitivity coefficients for $\sigma_{(n,\gamma)}$ of ^{238}U in total sensitivity analysis is larger than that in the explicit case and thus the implicit portions caused by $\sigma_{(n,\gamma)}$ of ^{238}U play positive contributions in the total relative sensitivity coefficients.

Secondly, for σ_a of ^{235}U shown in Fig. 2(b), the contributions of implicit portions can be either positive or negative for different groups. This phenomenon should be explained by incorporating implicit contribution sects basic cross-sections of absorption cross-section include he resonant nuclides could interpolate due to $\sigma_{(n,f)}$ and $\sigma_{(n,\gamma)}$ of ^{235}U. Within the resonance groups, the basic cross sections included in σ_a are only the $\sigma_{(n,f)}$ and $\sigma_{(n,\gamma)}$, because the others basic cross sections such as $\sigma_{(n,2n)}$ are the types of cross sections whose energy thresholds are up within the fast groups. For the total sensitivity analysis, both $\sigma_{(n,f)}$ and $\sigma_{(n,\gamma)}$ would be smaller than the ones in explicit sensitivity analysis, according to the explanation for $\sigma_{(n,\gamma)}$ of ^{238}U introduced above. Smaller $\sigma_{(n,f)}$ would result in smaller k_∞ and corresponding relative sensitivity coefficients in total sensitivity analysis, while smaller $\sigma_{(n,\gamma)}$ contributes on the contrary. Therefore the incorporated implicit contributions can be positive or negative shown in Fig. 2(b).

Thirdly, as to implicit contributions of $\sigma_{(n,\mathrm{elas})}$, the contributions are negative to the nuclides without resonance and positive to the nuclides with resonances. For the $\sigma_{(n,\mathrm{elas})}$ of nuclides without resonance, like ^{1}H and ^{16}O shown in Fig. 2(c) and Fig. 2 (d) respectively, the implicit portions play negative contributions to the total relative sensitivity coefficients. This phenomenon is reasonable from the neutron physics point of view. As to the explicit sensitivity analysis, when 1% positive relative perturbation has been added to $\sigma_{(n,\mathrm{elas})}$ of ^{1}H or ^{16}O, only $\sigma_{(n,\mathrm{elas})}$ of ^{1}H or ^{16}O would have 1% relative increase. However, for total sensitivity analysis, the perturbations would be added not only to $\sigma_{(n,\mathrm{elas})}$ of ^{1}H or ^{16}O, but also to the resonant cross sections within resonances groups. This is because that the dilution cross sections of system under analysis would become larger than that of the explicit situation due to increase in $\sigma_{(n,\mathrm{elas})}$ of ^{1}H or ^{16}O, so the resonant nuclides could interpolate larger fission yield and absorption cross sections. In the case of TMI pin-cell, $\sigma_{(n,f)}$, $\sigma_{(n,\gamma)}$ of ^{235}U and $\sigma_{(n,\gamma)}$ of ^{238}U in total sensitivity analysis would all become larger than those of the explicit sensitivity analysis. Moreover, according to Fig. 2(a) and Fig. 2(b), the implicit effects caused by incorporated $\sigma_{(n,f)}$ and $\sigma_{(n,\gamma)}$ of ^{235}U is over one order of magnitude smaller than that caused by $\sigma_{(n,\gamma)}$ of ^{238}U. In this context, the effect due to $\sigma_{(n,\gamma)}$ of ^{238}U would be dominant in this case. According to the explanation for $\sigma_{(n,\gamma)}$ of ^{238}U, the negative effect would be caused by increase in $\sigma_{(n,\gamma)}$ of ^{238}U. Therefore, the implicit portions of $\sigma_{(n,\mathrm{elas})}$ caused by nuclides without resonance paly negative contributions to the total relative sensitivity coefficients.

For $\sigma_{(n,\mathrm{elas})}$ of nuclides with resonances, the implicit portions paly positive contributions to the total relative sensitivity coefficients. For $\sigma_{(n,\mathrm{elas})}$ of ^{235}U and ^{238}U, the implicit contributions have the same presentation, shown as Fig. 2(e) for $\sigma_{(n,\mathrm{elas})}$ of ^{238}U. When $\sigma_{(n,\mathrm{elas})}$ of ^{235}U or of ^{238}U is larger, the resonance cross sections in the resonance tables would become smaller than the initial ones. The explanation for $\sigma_{(n,\gamma)}$ of ^{238}U and incorporated $\sigma_{(n,f)}$ and $\sigma_{(n,\gamma)}$ of ^{235}U introduced above can be applied here because increase in $\sigma_{(n,\mathrm{elas})}$ of nuclides with resonance would result in smaller fission yield and absorption cross sections. Since the effects caused by

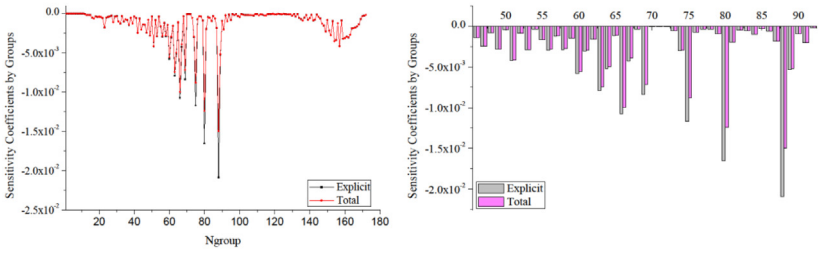

(a) Comparison of explicit and total relative sensitivity coefficients by groups for $^{238}U\ \sigma_{(n,\gamma)}$

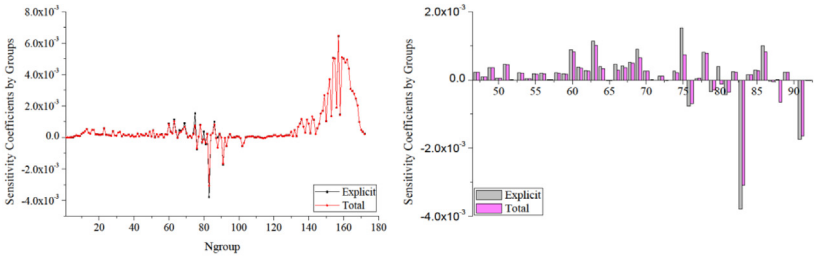

(b) Comparison of explicit and total relative sensitivity coefficients by groups for $^{235}U\sigma_a$

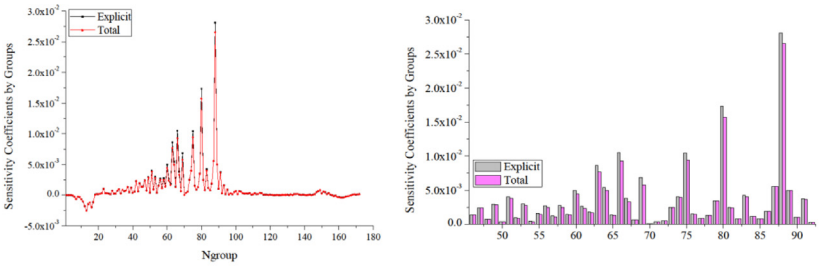

(c) Comparison of explicit and total relative sensitivity coefficients by groups for $^{1}H\ \sigma_{(n,elas)}$

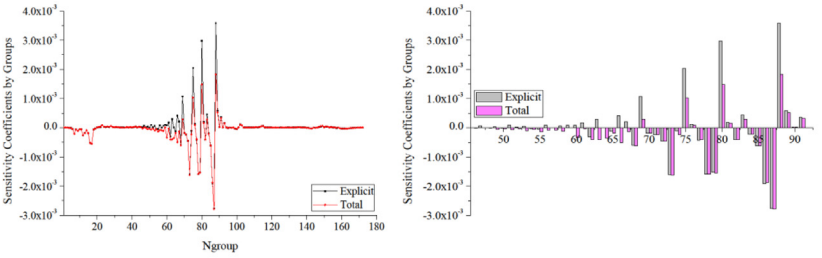

(d) Comparison of explicit and total relative sensitivity coefficients by groups for $^{16}O\ \sigma_{(n,elas)}$

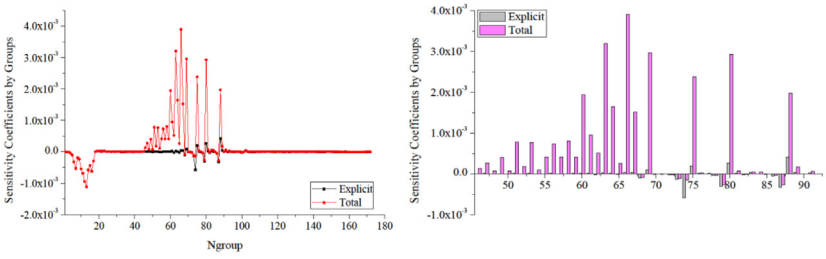

(e) Comparison of explicit and total relative sensitivity coefficients by groups for $^{238}U\sigma_{(n,elas)}$

Fig. 2. Comparisons of the explicit and total relative sensitivity coefficients by groups.

$\sigma_{(n,\gamma)}$ of ^{238}U would be dominant, thus on the contrary, smaller absorption cross section could result in larger k_∞ and corresponding relative sensitivity coefficients for total sensitivity analysis. Therefore, the implicit portions caused by $\sigma_{(n,elas)}$ of nuclides with resonance play positive contributions to the total relative sensitivity coefficients.

Table 6
The fifteen most significant relative uncertainties obtained by 20 different re-samples.

Nuclides	Parameter pair	DNP method	Statistical sampling method	
		$\sigma(k)/k/\%$	$\sigma(k)_0/k/\%$	$\Delta\sigma(k)/k/\%$
^{235}U	ν,ν	6.070E−01	5.933E−01	2.411E−02
^{235}U	$\sigma_{(n,f)}$, $\sigma_{(n,f)}$	7.851E−02	7.632E−02	2.706E−03
^{238}U	$\sigma_{(n,\gamma)}$, $\sigma_{(n,\gamma)}$	3.135E−01	3.059E−01	1.616E−02
^{1}H	$\sigma_{(n,\mathrm{elas})}$, $\sigma_{(n,\mathrm{elas})}$	3.391E−02	3.340E−02	1.553E−03
^{235}U	$\sigma_{(n,\gamma)}$, $\sigma_{(n,\gamma)}$	1.999E−01	1.959E−01	7.609E−03
^{238}U	ν,ν	7.045E−02	6.917E−02	2.320E−03
^{1}H	$\sigma_{(n,\gamma)}$, $\sigma_{(n,\gamma)}$	9.647E−02	9.420E−02	3.951E−03
^{238}U	$\sigma_{(n,f)}$, $\sigma_{(n,f)}$	1.472E−02	1.496E−02	1.673E−03
^{238}U	$\sigma_{(n,\mathrm{inel})}$, $\sigma_{(n,\mathrm{inel})}$	1.109E−01	1.090E−01	3.213E−03
^{91}Zr	$\sigma_{(n,\gamma)}$, $\sigma_{(n,\gamma)}$	2.176E−02	2.094E−02	9.546E−04
^{92}Zr	$\sigma_{(n,\gamma)}$, $\sigma_{(n,\gamma)}$	2.203E−02	2.041E−02	8.321E−04
^{90}Zr	$\sigma_{(n,\gamma)}$, $\sigma_{(n,\gamma)}$	1.729E−02	1.617E−02	7.025E−04
^{238}U	$\sigma_{(n,2n)}$, $\sigma_{(n,2n)}$	1.257E−02	1.347E−02	3.409E−03
^{16}O	$\sigma_{(n,\alpha)}$, $\sigma_{(n,\alpha)}$	8.410E−03	8.169E−03	3.152E−04
^{16}O	$\sigma_{(n,\mathrm{elas})}$, $\sigma_{(n,\mathrm{elas})}$	2.112E−02	2.322E−02	2.594E−03

6.2. Verification for total uncertainty analysis

In the previous section, it has been proven that the implementations of multigroup cross-section perturbation model and the DNP method are correct. Based on the multigroup cross-section perturbation model, the total uncertainty analysis has been performed, applying the statistical sampling method. And the covariance data of cross sections with 172 groups, used by both the DNP method and the statistical sampling method, is generated by NJOY from the ENDF/B-VII.1 library.

In this study, $nS = 300$ is selected as the size for each sample. In order to obtain much more confident uncertainty results, the bootstrap method is applied to quantify the confidence boundary for uncertainty results. Therefore, 20 different re-samples with size of 100 have been generated for total uncertainty analysis. The relative uncertainties of k_∞ due to the fifteen most significant uncertainty sources of cross sections for TMI-1 pin-cell are shown in Table 6. The uncertainty results of the statistical sampling method in Table 6 have been obtained by the 20 different re-samples.

In Table 6, the results obtained by the DNP method are calculated using "sandwich rule". The uncertainty results of the statistical sampling method include two parts: the expectation values for relative uncertainties of the 20 different re-samples, $\sigma(k)_0/k$, and the standard deviations of uncertainty results, $\Delta\sigma(k)/k$. Comparing the uncertainties by the DNP method and the statistical sampling method respectively, total uncertainty analysis by application of the statistical sampling method can be proved to be correct.

As shown in Table 6, the relative uncertainties of k_∞ introduced by basic cross sections are large and non-ignorable, which can reach up to 0.31% for $\sigma_{(n,\gamma)}$ of ^{238}U, 0.20% for $\sigma_{(n,\gamma)}$ of ^{235}U and 0.11% for $\sigma_{(n,\mathrm{inel})}$ of ^{238}U. These uncertainties wouldn't be shown if the detailed analysis hasn't been performed to the basic cross sections. Moreover, the total relative uncertainty of k_∞ due to the fifteen most significant uncertainties sources of cross sections is about 0.72% ± 0.031% by summing all the relative uncertainties of the fifteen most significant uncertainty sources in Table 6. This is such a large uncertainty which is significant to neutronics calculations.

7. Conclusions

In this paper, based on both the direct numerical perturbations method and the statistical sampling method, the UNICORN code has been developed to perform total sensitivity analysis and total uncertainty analysis for eigenvalue with respect to various basic multigroup cross sections. An improved multigroup cross-section perturbation model has been established for the purpose to consider the implicit effects and perform detailed analysis for basic cross sections. Moreover, the bootstrap method has been applied to the statistical sampling method to obtain much steadier and more confident uncertainty results.

The UNICORN code has been applied to perform total sensitivity analysis and total uncertainty analysis for TMI-1 pin-cell. Three aspects of conclusions can be obtained from the numerical results. Firstly, the implicit contributions are notable and non-ignorable. And the implicit contributions can be caused by $\sigma_{(n,\mathrm{elas})}$ of nuclides without resonance, and $\sigma_{(n,\mathrm{elas})}$,$\sigma_{(n,f)}$ and $\sigma_{(n,\gamma)}$ of nuclides with resonance. Secondly, the detailed analysis should be performed to basic cross sections. The uncertainties due to basic cross sections are significant and can reach up to be about 0.31%. Thirdly, the uncertainty analysis is essential for reactor physics. According to the total relative uncertainty due to the fifteen most significant uncertainty sources of cross sections to k_∞ of TMI-1 pin-cell, it is about 0.72%, which is non-ignorable for reactor physics calculations.

In further research plans, the responses will be extended to the others outputs such as few-group constants of assembly to propagate the uncertainties of input parameters to the assembly scale and even the core scale subsequently.

Acknowledgments

This work is supported by the National Natural Science Foundation of China No. 91126005, and by the National Natural Science Foundation of China No. 91226106.

References

Archer, G.E.B., Saltelli, A., Sobol, I.M., 1997. Sensitivity measures, anova-like techniques and the use of bootstrap. J. Stat. Comput. Simul. 58, 99–120.
Ball, M.R., Novog, D.R., Luxat, J.C., 2013. Analysis of implicit and explicit lattice sensitivity using DRAGON. Nucl. Eng. Des. 265, 1–12.
Broadhead, B.L., Rearden, B.T., Hopper, C.M., Wagschal, J.J., Parks, C.V., 2004. Sensitivity- and uncertainty-based criticality safety validation techniques. Nucl. Sci. Eng. 146, 340–366.
Dion, M., Marleau, G., 2013. Resonance Self-shielding Effects on Eigenvalue Sensitivity. M&C, Idaho, USA.
Foad, B., Takeda, T., 2015. Sensitivity and uncertainty analysis for UO2 and MOX fueled PWR cells. Ann. Nucl. Energy 75, 595–604.
Helton, J.C., Davis, F.J., 2002. Latin Hypercube Sampling and the Propagation of Uncertainty in Analysis of Complex System. Sandia National Laboratories, SAND2001-0417.
Helton, J.C., Johnson, J.D., Sallaberry, C.J., Storlie, C.B., 2006. Survey of sampling-based methods for uncertainty and sensitivity analysis. Reliab. Eng. Syst. Saf. 91, 1175–1209.
Ivanov, K., Avramova, M., Kamerow, S., Kodeli, I., Sartori, E., Ivanov, E., Cabellos, O., 2013. Benchmarks for Uncertainty Analysis in Modelling (UAM) for the Design, Operation and Safety Analysis of LWRs. OECD Nuclear Energy Agency, NEA/NSC/DOC(2013)7.
Kinoshita, K., Yamamoto, A., Endo, T., 2014. Uncertainty Quantification of BWR Core Characteristics Using Latin Hypercube Sampling Method. PHYSOR 2014, Kyoto, Japan.
Leszczynski, F., Aldama, D.L., Trkov, A., 2007. WIMS-D Library Update: Final Report of a Coordinated Research Project. International Atomic Energy Agency.
Liu, Y., Cao, L., Wu, H., Zu, T., Shen, W., 2015. Eigenvalue implicit sensitivity and uncertainty analysis with the subgroup resonance-calculation method. Ann. Nucl. Energy 79, 18–26.
Macfarlane, R.E., Muir, D.W., Boicourt, R.M., Kahler, A.C., 2012. The NJOY Nuclear Data Processing System, Version 2012. Los Alamos National Security, LA-UR-12-27079.
Marleau, G., Hébert, A., Roy, R., 2014. A User Guide for DRAGON Version 4. Technical Report, IGE-294.
Pusa, M., 2012. Incorporating sensitivity and uncertainty analysis to a lattice physics code with application to CASMO-4. Ann. Nucl. Energy 40, 153–162.
Rearden, B.T., 2009. TSUNAMI-1D: Control Module for One-dimension Cross-section Sensitivity and Uncertainty Analysis for Criticality. Nuclear Science and Technology Division, vol. I, Sect. C8.
Rearden, B.T., Jessee, M.A., 2009. TSUNAMI Utility Modules. Nuclear Science and Technology Division, vol. III, Sect. M18.

Rearden, B.T., Williams, M.L., James, E.H., 2005. Advances in the TSUNAMI Sensitivity and Uncertainty Analysis Codes Beyond SCALE 5.
Rearden, B.T., Petrie, L.M., Jessee, M.A., 2009. SAMS: Sensitivity Analysis Nodule for SCALE. Nuclear Science and Technology Division, vol. II, Sect. F22.
Weisbin, C.R., Marable, J.H., Lucius, J.L., Oblow, E.M., Mynatt, F.R., Peelle, R.W., Perey, F.G., 1976. Application of FORSS Sensitivity and Uncertainty Methodology to Fast Reactor Benchmark Analysis. Oak Ridge National Lab, ORNL/TM-5563.
Wieselquist, W., Vasiliev, A., Ferroukhi, H., 2012. Nuclear Data Uncertainty Propagation in a Lattice Physics Code Using Stochastic Sampling. PHYSOR 2012, Tennessee, USA.
Yankov, A., Klein, M., Jessee, M.A., Zwermann, W., Velkov, K., Pautz, A., Collins, B., Downar, T., 2012. Comparison of XSUSA and "Two-step" Approaches for Full-core Uncertainty Quantification. PHYSOR 2012, Tennessee, USA.